# Plasmalemma Transport of OH⁻ in *Chara corallina*

## III. FURTHER STUDIES ON TRANSPORT SUBSTRATE AND DIRECTIONALITY[1]

WILLIAM J. LUCAS
*Department of Botany, University of California Davis, California, 95616*

JACK M. FERRIER
*Department of Botany, University of Toronto, Toronto, Ontario M5S 1A1 Canada*

## ABSTRACT

The identity of the plasmalemma-transported species that develops the alkaline bands of *Chara corallina* was investigated. The effect of fusicoccin on the rate of $HCO_3^-$ assimilation, and on the time-dependent alkaline band pH buildup following low pH flushing, was found to be small, with no stimulatory effect. Computer simulation of the flushing experiments showed that in the experimental situation the alkaline band transport system was slowed down, rather than speeded up, by low pH flushing. A detailed theoretical examination of the maximum rate of proton production from water showed that measured alkaline band fluxes are too large to be explicable in terms of an $H^+$ influx system. The experimental and theoretical results indicate that the plasmalemma transport of $OH^-$ ions is responsible for the measured negative external electric potential and alkalinity flux which are associated with the alkaline band phenomenon. Consequently, $HCO_3^-$ influx across the characean plasmalemma must be charge-balanced by the efflux of $OH^-$ ions.

Following the inception of the Chemiosmotic theory (12, 13) numerous plant transport systems have been linked with the vectorial movement of protons across various membranes (14). In these transport systems it is assumed that $H^+$ is the chemical species which moves, not $OH^-$. In line with this general philosophy, Walker and Smith (16) suggested that the light (photosynthetic)-dependent alkalinity that develops on the cell wall surface of *C. corallina* (4) is formed by $H^+$ influx, via the operation of a simple $H^+$ uniport.

Recently Lucas (5) presented evidence which, although it did not categorically refute the existence of a $H^+$ influx system, tended to offer stronger support for the $OH^-$ efflux hypothesis. Supporting evidence against the operation of a $H^+$ uniport was claimed based on the very low $K_m$ requirement of such a system (nM range). Also, the apparent insensitivity of the alkalinization process to external pH (from 10 down to 5.0) was thought to be inconsistent with the operation of a $H^+$ uniport.

To study the synchronization mechanism which functions in these giant algal cells to integrate $HCO_3^-$ influx and the necessary charge-balancing transport process (6), it would be of advantage to know the chemical nature of the charge-balancing species. This study was conducted to test whether, physicochemically, exogenous $H^+$ ions could fill this charge-balancing role. As a result of these studies we are now almost certain that $HCO_3^-$ influx is charge-balanced by $OH^-$ efflux.

## MATERIALS AND METHODS

**Culture Material.** Culture material of *Chara corallina* Klein ex Willd., em. R.D.W. (= *Chara australis* R. Br.) was grown in the laboratory under artificial light. Cells were cut from the culture 16 h prior to use in an experiment. During this recovery period cells were bathed in a pretreatment solution containing (mM): NaCl, 1.0; KCl, 0.2; CaSO₄, 0.2; and NaHCO₃, 0.5 (initial pH 7.7).

**Photosynthetic $H^{14}CO_3^-$ Assimilation.** Assimilation of exogenous $H^{14}CO_3^-$ was measured using radioactive $NaH^{14}CO_3^-$ (New England Nuclear, sterile aqueous solution). These experiments were performed in the manner detailed by Lucas and Dainty (7). Individual experimental details are given in the text.

**pH Measurement of Alkaline Band Activity.** The pH values along the cell surface of *C. corallina* internodal cells were measured using the procedures of Lucas and Smith (9) and Lucas and Dainty (7). For experiments in which FC[2] was employed, cells were mounted in a small Plexiglas chamber instead of an agar diffusion block.

**Numerical Analysis Modeling.** Various theoretical pH profiles were obtained using the expanded numerical analysis (diffusion) program of Ferrier and Lucas (2). These programs were run on an IBM 370 Computer (University of Toronto).

## RESULTS

**Influence of FC on $HCO_3^-$ Assimilation.** Marrè has suggested that FC stimulates $H^+$ efflux in the Characeae (10, 11). If Walker and Smith (16) are correct, in that the light-dependent alkaline bands are produced by an $H^+$ influx system, it may be that the $H^+$ efflux and influx transport systems of the Characeae are identical in all respects except for their spatial location on the plasmalemma and their direction of net transport. If this were so, FC may well act to stimulate the alkaline band transport system; stimulation of $H^+$ influx would result in increased alkalinity at the cell surface.

This possibility was investigated using the isolating chamber technique developed by Lucas (5). In these experiments, 0.5 mM exogenous $HCO_3^-$ was employed (apparent $K_m$ for assimilation) to ensure the alkaline band transport system was operating well below saturation. The response of an alkaline band to ethanol (0.5%) and ethanol plus 10 μM FC-containing solutions is typified by the data presented in Figure 1. Provided the isolating chamber solution contained $HCO_3^-$, the alkaline band transport system was

[2] Abbreviations: CPW/B: *Chara* pond water containing added bicarbonate; FC: fusicoccin.

not perturbed by the introduction of 0.5% ethanol. The addition of FC did not elicit a consistent response in terms of affecting transport activity (Fig. 1). We found that the presence of FC frequently caused the transport center to migrate (Figs. 1 and 2). The same type of FC response was observed when $HCO_3^-$ was excluded from the isolating chamber solution (data not shown). The variability of the results and the FC-induced mobility of the band center limited the usefulness of the isolating chamber technique.

The effect of exposing entire internodal cells to FC was examined. In these experiments, internodal cells of varying maturation
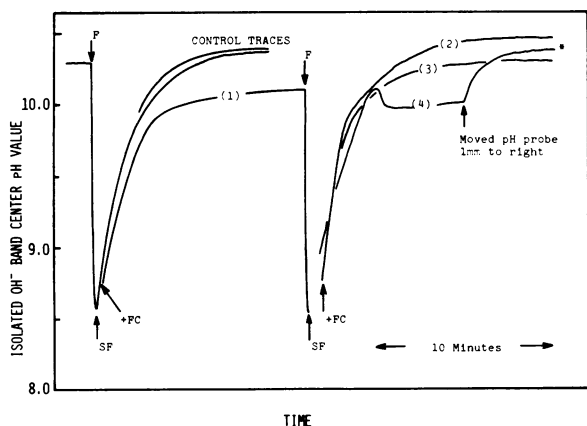


FIG. 1. Influence of ethanol and FC on the alkaline band transport system of *C. corallina*. Isolating chamber located over operational transport site and then cell allowed 30-min recovery, bathed in a solution containing (mM) 1.0 NaCl, 0.2 KCl, 0.2 CaSO₄, 0.5 NaHCO₃ (30 w m⁻² light intensity) [CPW/B]. Solution within the isolating chamber was changed (F: chamber flush) to CPW/B plus 0.5% ethanol (SF: end of flushing sequence). After repeating this treatment, the isolating chamber solution was replaced by CPW/B + 0.5% ethanol + 10 μM (+FC). Four FC recovery responses were obtained (*, rechecked band center and verified its position approximately 1 mm from previous location).
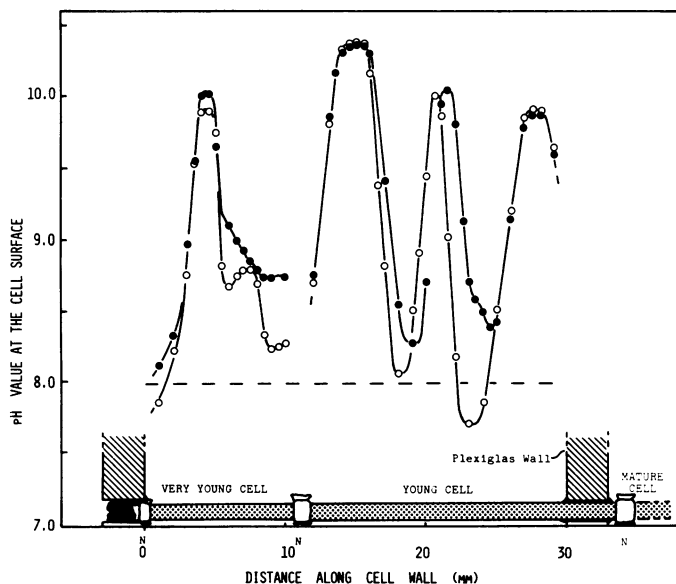


FIG. 2. Effect of FC on the light-dependent pH pattern established on the cell surface of *C. corallina*. Cells were bathed in CPW/B (20 w m⁻²) for 1 h before being scanned (data not shown). The CPW/B + 0.5% ethanol (○) and CPW/B + 0.5% ethanol + 10 μM FC (●) scans were also conducted after 1 h pre-equilibration. -----, Represents the pH value of the background solutions; N, represents the nodal location.

were employed. This approach gave consistent results. In all experiments in which young or mature cells were used, alkaline band transport activity was not enhanced by FC. This was also the case for very young cells, and the response shown in Figure 2 was selected because it was the largest effect obtained for all cells studied.

In the presence of FC, the steady state pH values in the regions between the alkaline bands were always more alkaline compared with the control situation. Inasmuch as this region is thought to be involved in $HCO_3^-$ transport (2), the possible influence of FC on $H^{14}CO_3^-$ assimilation was studied. Table I indicates that 10 and 20 μM FC had a slight inhibitory effect on net $H^{14}CO_3^-$ assimilation. However, when $K^+$ was either absent or present at higher than control levels, 20 μM FC caused a slight stimulation of $H^{14}CO_3^-$ assimilation. The observed effects were all quite small, and it is doubtful whether they demonstrate a significant influence of FC on the $H^{14}CO_3^-$ assimilating processes ($HCO_3^-$ influx, in particular).

The pH scanning and $H^{14}CO_3^-$ assimilation data do not provide support for the hypothesis that an $H^+$ influx system is responsible for the formation of the alkaline bands of *Chara*. The present data are also at variance with the proposal that FC stimulates $H^+$ efflux in the Characeae (10, 11).

**Computer Simulation of pH Pulse Experiments.** Lucas (5) suggested that if localized $H^+$ influx systems were generating the alkaline bands, it should be possible to saturate the carriers involved by exposing the localized site to low pH values. Under this substrate-saturation condition, it was suggested that the redevelopment of alkalinity (on the cell surface) would be delayed, due to the enhanced level of available substrate ($H^+$). However, no such delay was observed experimentally (5).

The validity of this delay hypothesis was investigated using our numerical analysis computer model (2, 8). The basic mechanics of the program remained unaltered except that we expanded the treatment to account for the diffusion of $OH^-$ away from, and $H^+$ toward, the alkaline band site. The flushing solutions did not contain $HCO_3^-$, hence, the numerical analysis program did not have to include the $HCO_3^-$ buffering effect. We simply simulated the pH flushing technique, whereby the $OH^-$ diffusion gradient established near the cell wall surface (by the alkaline band) was eliminated, and replaced by a new solution having a low pH value (5.0–7.0). In these studies a 100-μm spatial increment was used for the diffusion calculations. During the simulation, chemical equilibrium between $H^+$, $OH^-$, and $H_2O$ was imposed within the 100-μm volume element every 0.5 s.

As a control we examined the response of a simulated $OH^-$ efflux system to this external pH change. When the same program was run, except that $H^+$ ions were pumped into the cell (at a rate identical to that used for the $OH^-$ efflux program), an identical recovery pH response was generated (Fig. 3). A delay in the reestablishment of alkalinity was absent in both simulations. These

Table I. *Effect of Fusicoccin on $H^{14}CO_3^-$ Assimilation in C. corallina*

Control cells were pretreated for 30 min in a solution containing (mM): 1.0 NaCl, 0.2 KCl, 0.2 CaSO₄, 0.5 NaHCO₃ ([pH 9.0] 25 C and 20 wm⁻²) followed by 1 h ¹⁴C exposure. All other treatments were identical except the control solution which was modified as indicated.

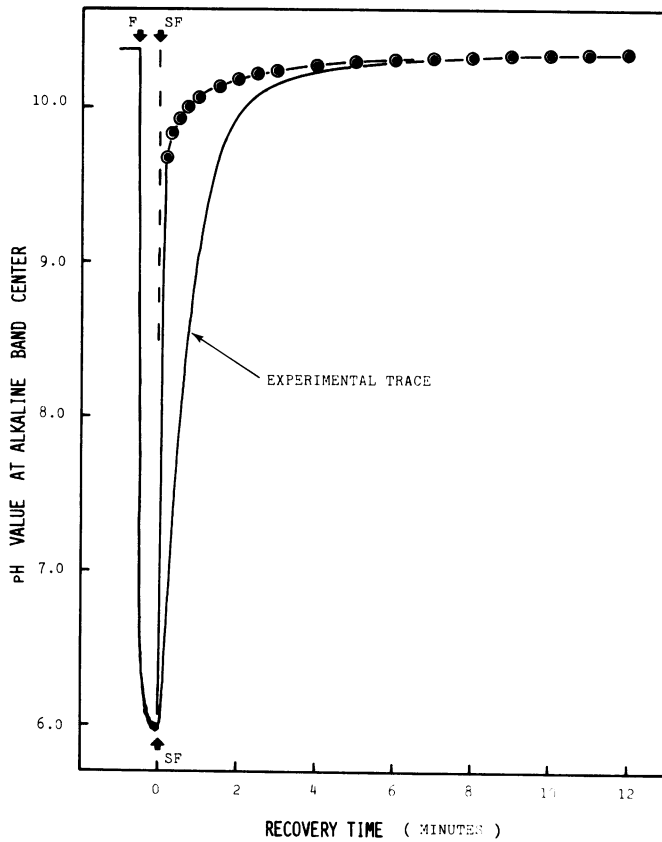| Treatment | Net $H^{14}CO_3^-$ Assimilation | Control |
|---|---|---|
| | *pmol cm⁻² s⁻¹* | *%* |
| Control | 27.6 ± 1.7 | |
| +0.5% (v/v) Ethanol | 27.9 ± 2.1 | 100 |
| +0.5% Ethanol + 10 μM FC | 25.0 ± 2.03 | 91 |
| +0.5% Ethanol + 20 μM FC | 24.7 ± 2.25 | 90 |
| +0.5% Ethanol + 20 μM FC − KCl | 30.8 ± 1.62 | 111 |
| +0.5% Ethanol + 20 μM FC + 0.5 mM KCl | 30.4 ± 1.78 | 110 |

FIG. 3. Experimental and simulated recovery pH traces generated following the elimination of the $OH^-$ diffusion pattern, established near the cell surface by the alkaline band transport system. In the experimental situation the diffusion pattern was eliminated by flushing new solution into the chamber (solution composition (mM): 1.0 NaCl, 0.2 KCl, 0.2 $CaSO_4$). F and SF represent the commencement and cessation of this flushing procedure, respectively. In the numerical analysis program the diffusion pattern was eliminated by resetting the pH values in all the spatial increments to the predetermined value (pH 6.0 in the case illustrated). The symbol (○) represents a simulated recovery response in which $OH^-$ ions were the transported species and the $OH^-$ efflux within the band center was 100 pmol $cm^{-2}$ $s^{-1}$. ●, Represents an identical computer simulation, except that $H^+$ ions were transported into the cell, with an equivalent band-center influx value.

results appear to invalidate the delay hypothesis proposed by Lucas (5).

The data in Figure 3 also indicate that for comparable steady-state fluxes, the pH responses obtained by computer simulation were more rapid than the experimental situation. Since we adjusted the steady-state experimental and simulation fluxes to the same value, this difference most probably reflects a slight perturbation of the characean alkaline band transport system during the flushing sequence.

**Chemical $H^+$ Production.** The accuracy of the numerical analysis data obtained for $H^+$ influx will depend to a marked degree on whether a suitable spatial increment was employed in the program and on whether a reasonable limit was placed on the rate of proton production within these spatial increments. We investigated this aspect by examining the kinetics of $H_3O^+$ production from $H_2O$.

An estimate of the maximum possible rate of $H^+$ influx at the plasmalemma surface can be obtained in the following manner. The net rate of $H_3O^+$ production from $H_2O$ per unit volume of solution $(Q_r)$ can be written as:

$$Q_r = k_f[H_2O]^2 - k_b[H_3O^+][OH^-] \qquad (1)$$

where $k_f$ ($5 \times 10^{-7}$ $mol^{-1}$ liter $s^{-1}$) and $k_b$ ($1.3 \times 10^{11}$ $mol^{-1}$ liter $s^{-1}$) are the forward and backward rate coefficients, respectively, for the dissociation of water (3). By continuity we can write, at steady-state:

$$Q_r = -D_H \cdot \nabla^2[H_3O^+] \qquad (2)$$

where $D_H$ is the proton diffusion coefficient (positive sign, of $H^+$, omitted to avoid confusion within the equations).

An absolute upper limit for $Q_r$ can be obtained by dropping the back reaction term in equation 1. Also, near the plasmalemma surface, the $H^+$ ($OH^-$) gradient will closely approximate that of a one-dimensional diffusion system. By employing these conditions, equations 1 and 2 can be combined to give:

$$-C''(x) = k_f[H_2O]^2/D_H$$

or
$$\qquad (3)$$

$$-C''(x) = K$$

where $C = [H_3O^+]$, $K = k_f[H_2O]^2/D_H$, and a prime sign indicates partial differentiation with respect to $x$, the distance from the plasmalemma.

Integration of equation 3 yields:

$$C(x) = -(K/2)x^2 + C'(O)x + C(O) \qquad (4)$$

where $C(x)$ is the proton concentration at $x$, and $C(O)$ and $C'(O)$ are, respectively, the proton concentration and gradient at the plasmalemma surface.

Equation 4 can be rearranged to give:

$$C'(O) = \{C(x) - C(O)\}/x + (K/2)x \qquad (5)$$

Now the proton flux at $x = 0$ is given by:

$$J_H(O) = -D_H \cdot C'(O) \qquad (6)$$

To obtain a solution for equation 6 it was necessary to determine the upper limit for $C'(O)$. To achieve this solution for equation 5 we had to establish realistic boundary limits and conditions. This entailed setting an upper limit for $x$ (i.e. $x_{max}$) and performing a sensitivity analysis with respect to $C(O)$ and $C(x_{max})$.

An initial value for $x_{max}$ was estimated by invoking the following condition: proton half-life = proton diffusion time to the plasmalemma. For a second order reaction where one reactant is present in excess, the half-life of the reaction $(\tau)$ is given by the equation:

$$\tau = -\ln 2/k_b(a - b) \qquad (7)$$

where a and b are the initial reactant concentrations. In this situation where (b ≫ a) equation 7 reduces to:

$$\tau_a = \ln 2/k_b(b) \qquad (8)$$

This is the case in our experimental system, where the steady state pH values (at the cell surface) range from 10 to 10.5; hence, $[OH^-] \gg [H^+]$.

Since an approximate diffusion time for a one-dimensional system is given by:

$$T = x^2/2D \qquad (9)$$

equations 8 and 9 can be combined to give a first order upper limit for $x$. Thus:

$$x_{max} = \{2D_H\ln 2/k_b[OH^-]\}^{1/2} \qquad (10)$$

Equations 5 and 10 were substituted into equation 6 and values for $J_H(O)_{max}$ calculated for a range of $C(x_{max})$ values. [The value of $C(O)$ was held constant at $10^{-14}$ mol $liter^{-1}$.]

Data pertinent to these calculations are presented in Table II. Theoretical concentration profiles that would be established for

Table II. *Physico-chemical Limits to the Production and Supply (by Diffusion) of $H_3O^+$ to a Putative $H^+$ Influx System in the Plasmalemma of Chara corallina*

| $(H_3O^+)_{max}$ | $^{\tau}H_3O^+$ | $\chi_{max}$ | $C'(O)$ | $^JH_3O^+(O)_{max}$ |
|---|---|---|---|---|
| $mol\ liter^{-1}$ | $s$ | $cm \times 10^6$ | $mol\ liter^{-1}\ cm^{-1}$ | $pmol\ cm^{-2}\ s^{-1}$ |
| $10^{-10}$ | $5.33 \times 10^{-8}$ | $1.88\ (3.15)^a$ | $9.58 \times 10^{-5}\ (5.73 \times 10^{-5})$ | $3.22\ (5.33)$ |
| $10^{-9}$ | $5.33 \times 10^{-7}$ | $5.96\ (9.96)$ | $3.03 \times 10^{-4}\ (1.81 \times 10^{-4})$ | $10.2\ (16.8)$ |
| $10^{-8}$ | $5.33 \times 10^{-6}$ | $18.9\ (31.5)$ | $9.58 \times 10^{-4}\ (5.73 \times 10^{-4})$ | $32.2\ (53.3)$ |

[a] Values were calculated using equations 5, 6 and 10 and $[H_3O^+](O)$ of $10^{-14}$ mol liter$^{-1}$. Solutions to equations obtained using $D_{H^+}^o$ (self diffusion coefficient, $9.308 \times 10^{-5}$ cm$^2$ s$^{-1}$) are given in parenthesis, all other solutions were obtained using $D_{HCl}^l$ (limiting diffusion coefficient, $3.335 \times 10^{-5}$ cm$^2$ s$^{-1}$).
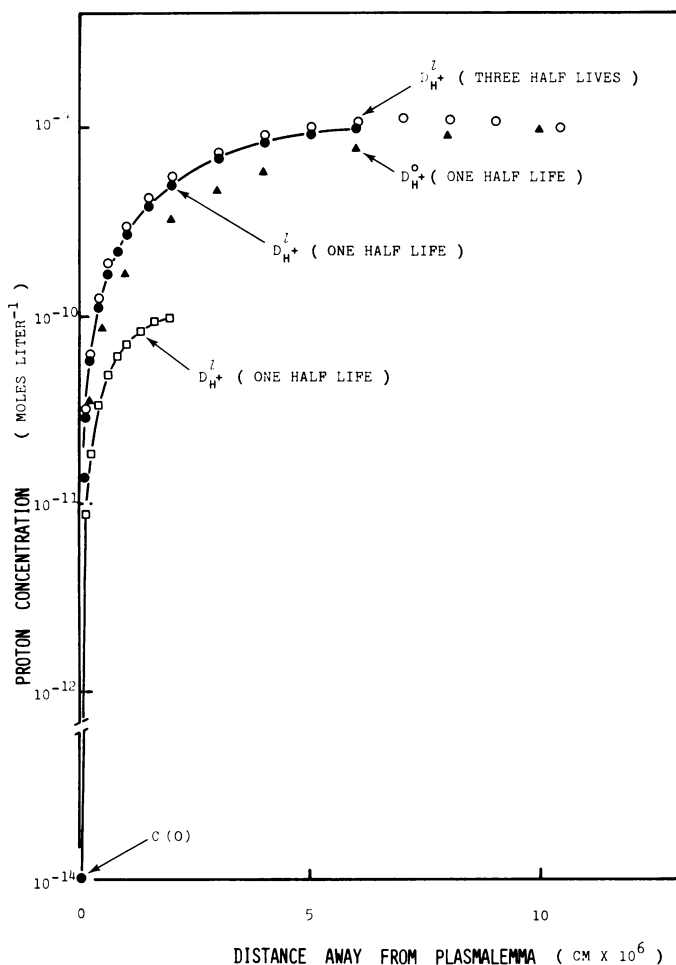


FIG. 4. Theoretical $H^+$ concentration profiles generated from equations 4, 5 and 10. The symbols $D_{H^+}^l$ and $D_{H^+}^o$ represent values computed using the limiting and self diffusion coefficients for protons, respectively.

different $C(x_{max})$ and $D_H$ values are also illustrated in Figure 4. The values obtained for $x_{max}$ indicate that the 100 $\mu$m diffusional increment used in the numerical analysis program was too large for $H^+$ calculations by several orders of magnitude. The computer program also allowed an unlimited rate of $H_3O^+$ production from water. The values obtained for the maximum proton flux were dependent upon the diffusion coefficient employed (Table II). However, irrespective of whether the limiting or the self diffusion coefficient was used, the maximum theoretical computed $H^+$ influx was smaller than the range of values obtained from diffusion studies (100–300 pmol cm$^{-2}$ s$^{-1}$; see Table I in ref. 8).

**Possible Electrophoretic Contributions.** There are two sources of electric fields that could also conceivably help to drive the putative (theoretical) proton influx. These fields originate from the fixed changes on the outer plasmalemma surface, and also as

a result of ionic fluxes that are being carried by self diffusion (2).

The Debye length ($\lambda$) for the field resulting from the plasmalemma surface charge can be calculated by Gouy-Chapman theory, provided that the surface potential is not too high. (This procedure will overestimate the potential gradient away from the plasmalemma because the theory ignores the existence of surface-adsorbed ions.) In the present study, $\lambda$ was calculated using the following equation:

$$\lambda = [(\kappa\epsilon_0 RT)/(F^2 \Sigma_i C_i Z_i^2)]^{1/2} \qquad (11)$$

where $\kappa$ is the dielectric coefficient of the solution, $\epsilon_0$ the permittivity of the free space, R the gas constant, T the absolute temperature, F the Faraday, and $\Sigma_i C_i Z_i^2$ is the ionic strength of the wall solution. To determine a value for the wall solution ionic strength, we assumed a Donnan potential of $-60$ mv. This gave $\Sigma_i C_i Z_i^2$ equal to 97 mM (using the standard ionic strengths employed in the experimental bathing solutions). Substitution of this value (97 mM) into equation (11) gave a $\lambda$ value of 1.4 nm.

Under our present conditions and assumptions the value of the surface potential can be calculated from the equation:

$$\psi(o) = \lambda q/\kappa\epsilon_0 \qquad (12)$$

where q is the surface charge density. Using $-8 \times 10^{-7}$ coulombs cm$^{-2}$ as a reasonable estimate for q (1) a value of $\psi(o) = -16$ mv was obtained. This value is low enough that the Debye length is a meaningful quantity, and we can write:

$$\psi'(x) = \psi'(o) \exp(-\chi/\lambda) \qquad (13)$$

where $\psi'(o)$ is the electric potential gradient at the membrane surface, given by:

$$\psi'(o) = q/\kappa\epsilon_0 \qquad (14)$$

Using the given value for q, $\psi'(o)$ would be $10^5$ v cm$^{-1}$. At a distance $7\lambda$ away from the membrane (9.8 nm), $\psi'(x)$ would be reduced to 100 v cm$^{-1}$.

The electrically driven (electrophoretic) proton flux at this distance would then be given by:

$$J_H(x) = -(D_H F/RT)\ C(x)\psi'(x) \qquad (15)$$

Using the self diffusion coefficient for protons, C (9.8 nm) equal to $10^{-12}$ mol cm$^{-3}$ and a $\psi'$ (9.8 nm) of 100 v cm$^{-1}$, one obtains an electrophoretic proton flux $[J_H$ (9.8 nm)] of 0.4 pmol cm$^{-2}$ s$^{-1}$. A comparison of this value with the diffusion-mediated fluxes presented in Table II indicates that this surface-potential electrophoretic flux could not make a significant contribution to the total putative proton flux.

Electrogenic transport of either $H^+$ into, or $OH^-$ out of, the *Chara* cell will establish a negative electric potential gradient within the external cell wall solution (2, 16). To determine the electrophoretic effect that this electric potential gradient would have on the total putative $H^+$ influx requires that we know the magnitude of this potential gradient ($\psi_e'$). The following equation, derived by Ferrier and Lucas (2), gives the relationship between

the electric and proton activity gradients:

$$\psi_e' = (RT/F)C'(x)/\Sigma_i C_i Z_i^2. \tag{16}$$

The ratio of the electrophoretic and self diffusion fluxes can be used to determine their relative importance. Hence:

$$\frac{J_{electrophoretic}}{J_{self\ diffusion}} = (D_H F/RT)C(x)\psi_e'(x)/D_H C'(x)$$
$$= C(x)/\Sigma_i C_i Z_i^2 \tag{17}$$

Substitution of $C(x) = 10^{-9}$ M and $\Sigma_i C_i Z_i^2 = 0.097$ M into equation 17 gives a flux ratio of $1.03 \times 10^{-8}$. Again we see that the flux contribution derived from this electric potential gradient would be negligible.

## DISCUSSION

At the center of alkaline bands, measured pH values can be as high as 10.5 (7). This represents a value measured slightly away from the cell wall surface. It is difficult to know exactly what the related value would be within the wall, or more pertinent to this analysis, what the pH would be against the plasmalemma surface. The Donnan potential of the cell wall, which may be as high as $-80$ mv (15), would have a definite effect on the $OH^-$ concentration within the wall. This effect may reduce the "local" pH of the wall from 10.5 to a value of approximately 9.0. However, it must be stressed that the distribution of these fixed negative charges within the wall is as yet not known. If the negative charge density of the wall is asymmetrically distributed such that the charges are concentrated near the plasmalemma, the negative charges may function as stabilizing sites for the protons produced from water. However, the $x_{max}$ values listed in Table II indicate that unless the majority of the negative charges are concentrated within the inner 0.2 $\mu$m of the wall, they would not play a direct role in reducing the back reaction of $H_3O^+$ and $OH^-$ to form $H_2O$.

A reliable value for $C(x_{max})$ within the wall solution is probably close to $10^{-10}$ mol liter$^{-1}$. Based on this value, the results presented in Table II clearly demonstrate that from a physico-chemical standpoint the maximum theoretical $H^+$ influx is much smaller than the range of experimentally observed fluxes. The values are too small by at least an order of magnitude.

At this point it should be stressed that the $J_{H_3O^+}$ values in Table II represent our attempt to obtain a theoretical absolute upper limit. Because the back reaction is not negligible (see $\tau_{H_3O^+}$ values in Table II), realistic $J_{H_3O^+}$ (max) values would be much smaller. Similarly, if we allowed for the physical effect of the cell wall material on both the effective proton diffusion coefficient and volume of water available in which the dissociation reaction could proceed, we would obtain flux values below those presented in Table II.

The values of $C(O)$ and $x_{max}$ have different degrees of influence on the calculations. The value of $C(O)$ was set at $10^{-14}$ mol liter$^{-1}$; firstly, because we wanted to set the value lower than known $pK_b$ values for an amino group, and secondly, values smaller than $10^{-14}$ had no further influence on $J_{H^+}$ (max). If $x_{max}$ is recalculated allowing for a three half-life situation, the value for $J_{H_3O^+}(O)$

changes from 10.2 (Tables II, $C(O) = 10^{-9}$ mol liter$^{-1}$) to 10.9 pmol cm$^{-2}$ s$^{-1}$. This change is almost insignificant, indicating that the determined values are not highly sensitive to the spatial conditions imposed.

This aspect can be examined another way. The observed fluxes associated with the center of the alkaline band often fall into the range of 150–200 pmol cm$^{-2}$ s$^{-1}$. Using a value of 150 pmol cm$^{-2}$ s$^{-1}$, $C'(O)$ would have to be $4.43 \times 10^{-3}$ mol liter$^{-1}$ cm$^{-1}$ (using $D_{H^+}'$ in the calculation). A value of 2 $\mu$m for $x_{max}$ would be obtained from equation 5. For a proton flux of this magnitude to occur, the $H_3O^+$ ions produced from the dissociation of water within this volume would have to be stabilized within this cell wall solution for a period in excess of 1,000 half-lives.

We feel that the present results indicate that from a physico-chemical standpoint, the alkalinity which develops on the surface of *Chara* internodal cells cannot be produced by a transport system moving $H^+$ from the cell wall solution to the cytoplasm. The evidence most strongly favors the existence of an $OH^-$ efflux system. However, there is one possibility that cannot be discounted. It is possible, theoretically, that the observed alkalinity is generated by a transport system that initially binds $H_2O$ and then splits this substrate, vectorially, into $H^+$ (influx) and $OH^-$ (diffuses away from the plasmalemma).

## LITERATURE CITED

1. ELUL R 1967 Fixed charge in the cell membrane. J Physiol 189: 351–365
2. FERRIER JM, WJ LUCAS 1979 Plasmalemma transport of OH⁻ in *Chara corallina*. II. Further analysis of the diffusion system associated with OH⁻ efflux. J Exp Bot 30: 705–718
3. FROST AA, RG PEARSON 1961 Kinetics and Mechanism. Ed 2. John Wiley & Sons, New York, pp 209–210
4. LUCAS WJ 1975 The influence of light intensity on the activation and operation of the hydroxyl efflux system of *Chara corallina*. J Exp Bot 26: 347–360
5. LUCAS WJ 1979 Alkaline band formation in *Chara corallina*: due to OH⁻ efflux or H⁺ influx? Plant Physiol 63: 248–254
6. LUCAS WJ 1980 Control and synchronization of HCO₃⁻ and OH⁻ transport during photosynthetic assimilation of exogenous HCO₃⁻. *In* RM Spanswick, WJ Lucas, J Dainty, eds, Membrane Transport in Plants: Current Conceptual Issues. Elsevier, Amsterdam, pp 317–330
7. LUCAS WJ, J DAINTY 1977 HCO₃⁻ influx across the plasmalemma of *Chara corallina*: divalent cation requirement. Plant Physiol 60: 862–867
8. LUCAS WJ, JM FERRIER, J DAINTY 1977 Plasmalemma transport of OH⁻ in *Chara corallina*: Dynamics of activation and deactivation. J Membr Biol 32: 49–73
9. LUCAS WJ, FA SMITH 1973 The formation of alkaline and acid regions at the surface of *Chara corallina* cells. J Exp Bot 24: 1–14
10. MARRÈ E 1978 Membrane activities as regulating factors for plant cell functions. Biol Cellulaire 32: 19–24
11. MARRÈ E 1979 Fusicoccin: a tool in plant physiology. Annu Rev Plant Physiol 30: 273–288
12. MITCHELL P 1966 Chemiosmotic coupling in oxidative and photosynthetic phosphorylation. Biol Rev 41: 445–502
13. MITCHELL P 1967 Translocations through natural membranes. Adv Enzymol 29: 33–87
14. POOLE RJ 1978 Energy coupling for membrane transport. Annu Rev Plant Physiol 29: 437–460
15. SPANSWICK RM, J STOLAREK, EJ WILLIAMS 1967 The membrane potential of *Nitella translucens*. J Exp Bot 18: 1–16
16. WALKER NA, FA SMITH 1977 Circulating electric currents between acid and alkaline zones associated with HCO₃⁻ assimilation in *Chara*. J Exp Bot 28: 119–120